



Structure mechanical modeling of thin-walled closed-section composite beams, part 2: Multi-cell cross section



S. Wang*, C. Zhang

Department of Aeronautical and Automotive Engineering, Loughborough University, Loughborough, Leicestershire LE11 3TU, UK

ARTICLE INFO

Article history:
Available online 13 March 2014

Keywords:
Closed-section
Composite beams
Multi-cell
Thin-walled

ABSTRACT

The methodology used in part 1 (Zhang and Wang, submitted for publication) of the work for single-cell thin-walled closed-section composite beams is extended to multi-cell thin-walled closed-section composite beams. The effect of material anisotropies is fully considered on the mid-surface shear strain of all the cross sectional members including skin walls and internal members. Numerical comparisons with ABAQUS finite element simulations are performed for three-cell box and elliptical beams with a variety of laminate layups under various loading conditions and excellent agreements are observed. Significant deficiency of some existing models are shown.

© 2014 Elsevier Ltd. All rights reserved.

1. Introduction

An accurate structure mechanical model has been developed in part 1 [1] of the work for TWCSBs with single-cell cross sections. In this part 2, the model is extended to TWCSBs with multi-cell cross sections which are much more popular in several industrial sectors. The extension will involve more complex analytical operations than that for TWCSBs with single-cell cross sections. All the kinematic developments remain the same and are not repeated here. However, details will be presented here to determine the local shell wall axial warping displacement, the mid-surface shear strain and the global beam stiffness matrix.

2. The TWCSBs model in [2–4]

Fig. 1 shows the multi-cell cross section of a TWCSB with its shear flow diagram. Although it is in a relatively simple one-direction multi-cell arrangement, the principle for the development of present 1-D TWCSB modeling will be thoroughly demonstrated and remains the same for any arbitrary multi-cell arrangements.

Eq. (13) in part 1 of the work [1] gives the local shell wall mid-surface warping displacement $\bar{w}_\omega(s, z)$ as

$$\bar{w}_\omega(s, z) = -\Phi'(z) \int_0^s r(s) ds + \int_0^s \bar{\gamma}_{sz} ds + \bar{w}_\omega(0, z) \quad (1)$$

with $\bar{w}_\omega(0, z) = C^{-1} \oint [\Phi'(z) \int_0^s r(s) ds - \int_0^s \bar{\gamma}_{sz} ds] ds$ and $C = \oint ds$. Note that the circular integration symbol \oint denotes an integration over the whole cross section perimeter including both the skin and internal shell walls and starting point $s = 0$ is arbitrary. It is seen from Eq. (1) that the shell wall mid-surface shear strain $\bar{\gamma}_{sz}$ needs to be determined first in order to determine the shell wall mid-surface axial warping displacement $\bar{w}_\omega(s, z)$. Applying Eq. (1) to any one complete cell, e.g. the R_{th} cell 1–2–3–4–1 as shown in Fig. 1, gives

$$\oint_R \bar{\gamma}_{sz} ds = 2A_{eR} \Phi'(z) \quad (2)$$

where $2A_{eR} = \oint_R r ds$ with A_{eR} being the enclosed area by the R_{th} cell. In order to determine $\bar{\gamma}_{sz}$, Librescu and Song [2] assumes a constant shear flow q_R developed within each cell under the St.Venant pure torque. Therefore, the resultant shearing force due to torsion on the four walls of the R_{th} cell are $N_{szT}^{12} = q_R$, $N_{szT}^{23} = q_R - q_{R-1}$, $N_{szT}^{34} = q_R$, $N_{szT}^{41} = q_R - q_{R+1}$, respectively. Further, the work [2] makes the same treatment as that for single-cell cross section. That is, $N_{sz} \approx N_{szT} = G(s, z) t(s, z) \bar{\gamma}_{sz}(s, z)$ where $G(s, z)$ is called the equivalent shear modulus and $t(s, z)$ is the thickness of the shell wall. However, it is not reported in the work [2] how to determine the equivalent shear modulus $G(s, z)$ in the case of generally laminated composite materials. Now, using the above two assumptions Eq. (2) becomes,

$$\Phi'(z) = \frac{1}{2A_{eR}} [q_R \delta_{12} + (q_R - q_{R-1}) \delta_{23} + q_R \delta_{34} + (q_R - q_{R+1}) \delta_{41}] \quad (3a)$$

where

$$\delta_{ij} = \int_i^j (ds/Gt) \quad (3b)$$

* Corresponding author. Tel.: +44 1509 227252.
E-mail address: S.Wang@lboro.ac.uk (S. Wang).

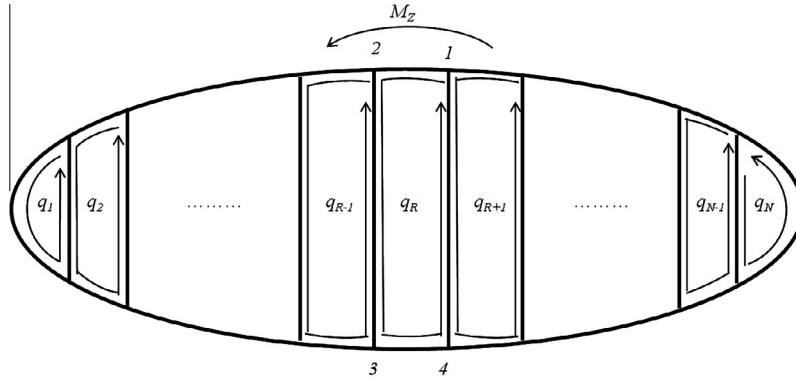


Fig. 1. A multi-cell cross section with its shear flow under pure torque M_z .

This can be rearranged as:

$$\Phi'(z) = \frac{1}{2A_{eR}}(-q_{R-1}\delta_{R,R-1} + q_R\delta_{R,R} - q_{R+1}\delta_{R,R+1}) \quad (4a)$$

where

$$\delta_{R,R-1} = \int_{R,R-1} (ds/Gt) \quad (4b)$$

$$\delta_{R,R} = \oint_{R,R} (ds/Gt) \quad (4c)$$

$$\delta_{R,R+1} = \int_{R,R+1} (ds/Gt) \quad (4d)$$

$\delta_{R,R-1}$ represents the integration on the wall bounded by the R_{th} cell and the $(R - 1)_{th}$ cell; $\delta_{R,R}$ denotes the closed integration on the R_{th} cell and $\delta_{R,R+1}$ represents the integration on the wall bounded by the R_{th} cell and the $(R + 1)_{th}$ cell. Assembling Eq. (4) for all the N cells shown in Fig. 1 gives

$$[H]\{q\} = \{I\}\Phi' \quad (5a)$$

where

$$\{q\} = \{q_1 \ q_2 \ \dots \ q_R \ \dots \ q_{N-1} \ q_N\}^T \quad (5b)$$

$$\{I\} = \{1 \ 1 \ \dots \ 1 \ \dots \ 1 \ 1\}^T \quad (5c)$$

$$[H] = \begin{bmatrix} H_{1,1} & -H_{1,2} & 0 & \dots & \dots & \dots & \dots & \dots & 0 \\ -H_{2,1} & H_{2,2} & -H_{2,3} & 0 & \dots & \dots & \dots & \dots & 0 \\ 0 & \dots & \dots & \dots & \dots & \dots & \dots & \dots & 0 \\ 0 & \dots & 0 & -H_{R,R-1} & H_{R,R} & -H_{R,R+1} & 0 & \dots & 0 \\ 0 & \dots & \dots & \dots & \dots & \dots & \dots & \dots & 0 \\ 0 & \dots & \dots & \dots & \dots & \dots & -H_{N-1,N-2} & H_{N-1,N-1} & -H_{N-1,N} \\ 0 & \dots & \dots & \dots & \dots & \dots & 0 & -H_{N,N-1} & H_{N,N} \end{bmatrix} \quad (5d)$$

where the elements H_{ij} are expressed as:

$$H_{ij} = \frac{1}{2A_{ei}}\delta_{ij} \quad (5e)$$

From Eq. (5), the shear flow of each cell, as a function of sectional rate of twist, $\Phi'(z)$, is given as

$$\{q\} = \{J\}\Phi' \quad (6a)$$

where

$$\{J\} = [H]^{-1}\{I\} \quad (6b)$$

Finally, the shear flow distribution in each wall can be calculated as:

$$\{q_1 \ q_{2,1} \ \dots \ q_R \ q_{R+1,R} \ \dots \ q_{N,N-1} \ q_N\}^T = \{J_1 \ J_2 - J_1 \ \dots \ J_R \ J_{R+1} - J_R \ \dots \ J_N - J_{N-1} \ J_N\}^T \Phi' \quad (7)$$

where the subscript of R denotes the walls of the R_{th} cell that are not bounded with any other cells, e.g. the wall 1–2 and 3–4 in Fig. 1. Whereas the subscript of $R + 1, R$ denotes the wall bounded by $(R + 1)_{th}$ and R_{th} cells, for example the wall 4–1 in Fig. 1. By using the earlier assumption $N_{sz} \approx N_{szT} = G(s, z)t(s, z)\bar{\gamma}_{sz}(s, z)$ the distribution of shell wall mid-surface shear strain for a multi-cell section in the work [2] becomes:

$$\begin{aligned} & \{\bar{\gamma}_{sz}^1 \ \bar{\gamma}_{sz}^{2,1} \ \dots \ \bar{\gamma}_{sz}^R \ \bar{\gamma}_{sz}^{R+1,R} \ \dots \ \bar{\gamma}_{sz}^{N,N-1} \ \bar{\gamma}_{sz}^N\}^T \\ & = \left\{ \begin{matrix} J_1/(Gt)_1 & (J_2 - J_1)/(Gt)_{2,1} & \dots & J_R/(Gt)_R & (J_{R+1} - J_R)/(Gt)_{R+1,R} & \dots \\ (J_N - J_{N-1})/(Gt)_{N,N-1} & J_N/(Gt)_N & & & & \end{matrix} \right\}^T \Phi' \end{aligned} \quad (8a)$$

Eq. (8a) can be written in a more compact form as

$$\bar{\gamma}_{sz}(s, z) = \psi(s)\Phi'(z) = \psi(s)K_{XY}(z) \quad (8b)$$

where the location of wall segments is represented as $s = (1), (2, 1), \dots, (R), (R + 1, R), \dots, (N, N - 1), (N)$. ψ is called the torsional function of a multi-cell closed-section.

Instead of assuming constant shear flow $N_{sz} \approx N_{szT} = G(s, z)t(s, z)\bar{\gamma}_{sz}(s, z)$ on each shell wall segment [2], the work [3,4] assumes a constant quantity $\bar{\gamma}_{sz}t$. The torsional function ψ in the work [3,4] therefore becomes:

$$\psi(s) = \{J_1/t_1 \ (J_2 - J_1)/t_{2,1} \ \dots \ J_R/t_R \ (J_{R+1} - J_R)/t_{R+1,R} \ \dots \ (J_N - J_{N-1})/t_{N,N-1} \ J_N/t_N\}^T \quad (9)$$

The δ integrations corresponding to Eqs. (4b)–(4d) change to be

$$\delta_{R,R-1} = \int_{R,R-1} (ds/t) \quad (10a)$$

$$\delta_{R,R} = \oint_{R,R} (ds/t) \quad (10b)$$

$$\delta_{R,R+1} = \int_{R,R+1} (ds/t) \quad (10c)$$

The mechanical meaning of constant quantity $\bar{\gamma}_{sz}t$ is unclear for composite materials.

Now, substituting Eq. (8b) into Eq. (1) gives the shell wall mid-surface axial warping displacement.

$$\bar{w}_\omega(s, z) = -\omega(s)\Phi'(z) \quad (11)$$

where $\omega(s) = \eta(s) - C^{-1} \int \eta ds$ is the warping function with $\eta(s) = \int_0^s [r(s) - \psi(s)] ds$. It has same form as that for single-cell cross section as expected. Then, the shell wall mid-surface axial strain $\bar{\epsilon}_{zz}$ is expressed as in terms of the global beam strain and curvatures, which is the same as that in Eq. (18) in part 1 [1] and is recorded here.

Download English Version:

<https://daneshyari.com/en/article/251568>

Download Persian Version:

<https://daneshyari.com/article/251568>

[Daneshyari.com](https://daneshyari.com)